Received: 22 February 2021 | Revised: 13 May 2021 | Accepted: 31 May 2021

DOI: 10.1002/mrm.28892

TECHNICAL NOTE

Magnetic Resonance in Medicine

Spirometry-based reconstruction of real-time cardiac MRI: Motion control and quantification of heart–lung interactions

Lena Maria Röwer[1,2] | **Tobias Uelwer**[3] | **Janina Hußmann**[1,2] | **Halima Malik**[1,2] | **Monika Eichinger**[4,5,6] | **Dirk Voit**[7] | **Mark Oliver Wielpütz**[4,5,6] | **Jens Frahm**[7,8] | **Stefan Harmeling**[3] | **Dirk Klee**[2] | **Frank Pillekamp**[1]

[1]Department of General Pediatrics, Neonatology and Pediatric Cardiology, University Children's Hospital Düsseldorf, Düsseldorf, Germany

[2]Department of Diagnostic and Interventional Radiology, Heinrich Heine University, Düsseldorf, Germany

[3]Department of Computer Science, Heinrich Heine University, Düsseldorf, Germany

[4]Department of Diagnostic and Interventional Radiology with Nuclear Medicine, Thoraxklinik, University of Heidelberg, Heidelberg, Germany

[5]Department of Diagnostic and Interventional Radiology, University Hospital of Heidelberg, Heidelberg, Germany

[6]Translational Lung Research Center Heidelberg, German Center for Lung Research, Heidelberg, Germany

[7]Biomedizinische NMR, Max-Planck Institute for Biophysical Chemistry, Göttingen, Germany

[8]Partner Site Göttingen, German Centre for Cardiovascular Research, Berlin, Germany

Correspondence
Frank Pillekamp, Department of General Pediatrics, Neonatology and Pediatric Cardiology, University Children's Hospital Düsseldorf, Medical Faculty, Moorenstr. 5, 40225 Düsseldorf, Germany.
Email: frank.pillekamp@hhu.de

Funding information
Elterninitiative Kinderkrebsklinik e.V.

Purpose: To test the feasibility of cardiac real-time MRI in combination with retrospective gating by MR-compatible spirometry, to improve motion control, and to allow quantification of respiratory-induced changes during free-breathing.

Methods: Cross-sectional real-time MRI (1.5T; 30 frames/s) using steady-state free precession contrast during free-breathing was combined with MR-compatible spirometry in healthy adult volunteers ($n = 4$). Retrospective binning assigned images to classes that were defined by electrocardiogram and spirometry. Left ventricular eccentricity index as an indicator of septal position and ventricular volumes in different respiratory phases were calculated to assess heart–lung interactions.

Results: Real-time MRI with MR-compatible spirometry is feasible and well tolerated. Spirometry-based binning improved motion control significantly. The end-diastolic epicardial eccentricity index increased significantly during inspiration (1.04 ± 0.04 to 1.19 ± 0.05; $P < .05$). During inspiration, right ventricular end-diastolic volume (79 ± 17 mL/m^2 to 98 ± 18 mL/m^2), stroke volume (41 ± 8 mL/m^2 to 59 ± 11 mL/m^2) and ejection fraction ($53 \pm 3\%$ to $60 \pm 1\%$) increased significantly, whereas the end-systolic volume remained almost unchanged. Left ventricular end-diastolic volume, left ventricular stroke volume, and left ventricular ejection fraction decreased during inspiration, whereas the left ventricular end-systolic volume increased. The relationship between stroke volume and end-diastolic volume (Frank-Starling relationship) based on changes induced by respiration allowed for a slope estimate of the Frank-Starling curve to be 0.9 to 1.1.

Conclusion: Real-time MRI during free-breathing combined with MR-compatible spirometry and retrospective binning improves image stabilization, allows quantitative image analysis, and importantly, offers unique opportunities to judge heart–lung interactions.

KEYWORDS

cardiac magnetic resonance imaging, computer-assisted methods, free-breathing examinations, heart diagnostic imaging, image processing, real-time imaging, respiration, spirometry

1 | INTRODUCTION

Physiological conditions in combination with the best available methods to quantify physiological parameters are necessary to judge heart–lung interactions and to guarantee meaningful cardiac function examinations. Noninvasive studies are preferred to investigations necessitating, for example, catheterization, sedation, or even anesthesia with mechanical ventilation because these interventions are known to interfere with cardiovascular function.

Similarly, free-breathing imaging better represents the physiological conditions compared with breath-hold imaging.[1,2] Breath-hold in expiration, but especially in inspiration, induces primarily neurally mediated heart-rate changes.[3,4] Breath-hold–induced alterations of preload and intrathoracic pressure modify ventricular size and stroke volume.[2]

Real-time MRI commonly uses radial data encoding combined with nonlinear inverse reconstruction to provide accelerated imaging.[5-7] It ensures significantly increased temporal resolution, whereas image quality (ie, spatial resolution and signal-to-noise ratio) is only slightly reduced.[5-7]

This fast imaging technique is perfectly suited for visualization and investigation of moving structures like the heart (see Zhang et al[8] for a review). It offers the opportunity to replace the conventional breath-hold technique by imaging during free-breathing.[9]

Spirometry is the gold standard to measure pulmonary ventilatory function and can be performed in concert with MRI.[10,11]

To ensure physiological conditions, we tested the feasibility of combining real-time MRI with simultaneous spirometry to assess cardiac function during free-breathing.

We hypothesized that this technique would enable good motion control and could ease semiautomated image analysis. In addition, we investigated the suitability of this combination for studying heart–lung interactions, that is, the influence of respiration on ventricular dimensions and function.

2 | METHODS

Adult healthy volunteers without contraindications ($n = 4$, aged 24–55 years (39 ± 14 years), body weight 72.5 ± 8.2 kg; two male, two female) signed a written consent form. The study was approved by the Ethics Committee of the Faculty of Medicine of Heinrich Heine University Düsseldorf (Study No: 6176R).

Real-time MRI with steady-state free precession (SSFP) contrast was used to acquire a short axis stack for volumetry (see Supporting Information S1 and Figure S1 for details).

Physiological data acquired by electrocardiogram (ECG), respiratory bellows, and MR-compatible spirometry were recorded continuously (see Supporting Information S1 and S2 for details). MR-compatible spirometry was performed as described by Eichinger et al[10] and as shown in Supporting Information Figure S2.

A questionnaire was used to assess anxiety and comfort during scanning (modified from Chen et al[12] (see Supporting Information S3).

2.1 | Binning

Binning of real-time MR images acquired during free-breathing was performed using the information provided by MR-compatible spirometry (flow and flow-derived lung volume) and ECG-derived distance between consecutive R-waves (RR interval) (Figure 1).

ECG-derived RR intervals were assigned to MR images by the intrinsic MR scanner software (Syngo MR E11; Siemens Healthineers). Respiratory information obtained by spirometry was assigned to the individual MR images after preprocessing using the programming language Python (Python Software Foundation), by adapting published open-source packages (eg, Numpy[13] and pydicom[14]; Figure 1A).

MR images were binned in eight respiratory classes (inspiration/expiration; four different lung volumes) and 25 cardiac phases (interval: 33.5 ± 4.3 ms; Figure 1B).

Images were selected and arranged focusing on heart cycle-dependency (eg, ventricular volume, ejection fraction or respiratory effects (eg, heart–lung interaction, eccentricity index [EI]; Figure 1C).

Binning was individualized by the typical tidal volume and heart rate observed to optimize the number of filled

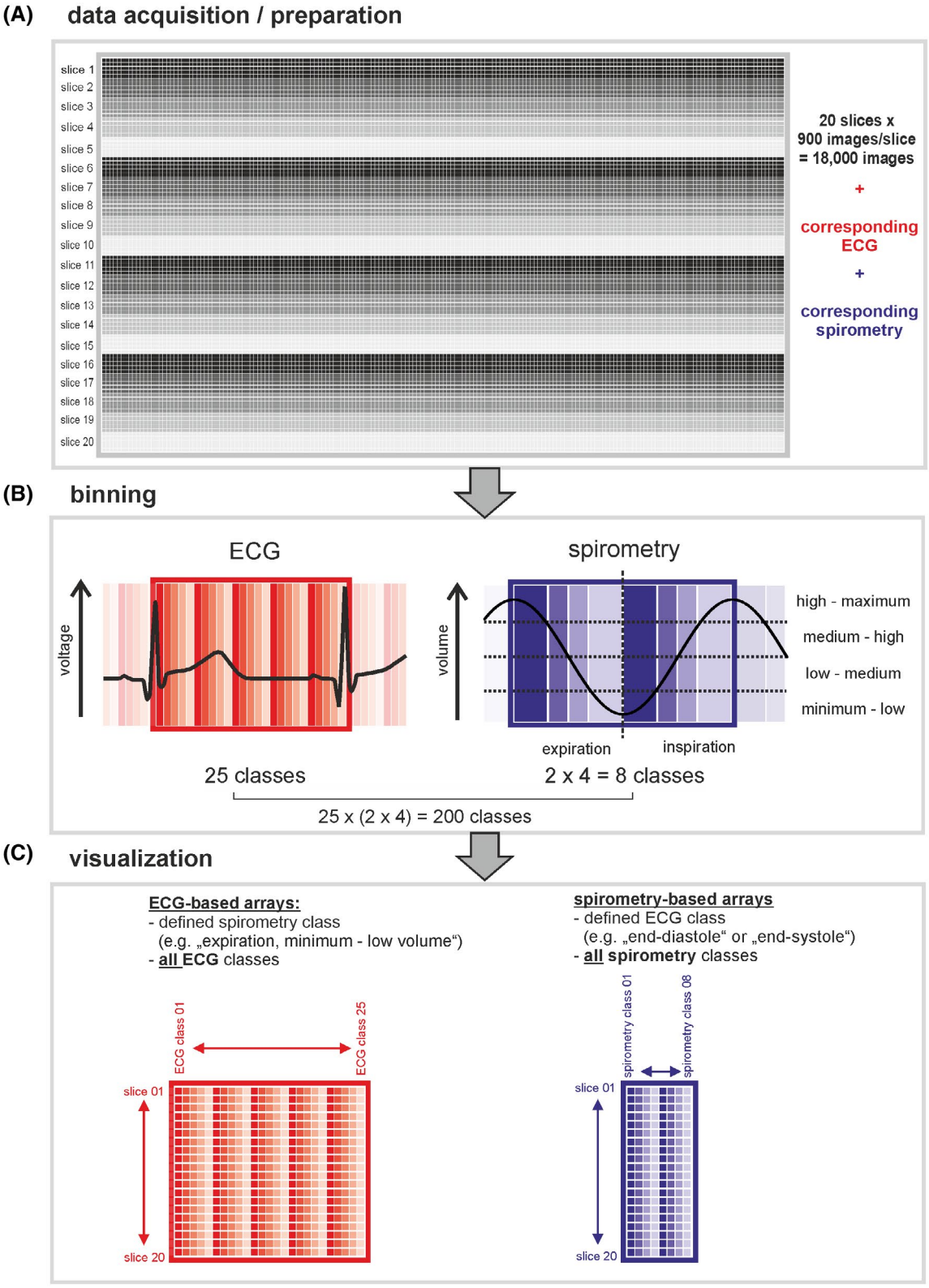

FIGURE 1 Binning. After assignment of respiratory and electrocardiogram (ECG) data to the real-time MR images (A), images were sorted into ECG and respiratory classes (B). Typically, ECG- or spirometry-based arrays were used for visualization and analysis (C)

bins. Unfilled bins were excluded from the analysis. In case of overfilled bins, the image closest to the median lung volume of the respiratory class was chosen.

Further analyses were performed with a commercial cardiac MR software [cvi42; Release 5.10.1.(1241); Circle Cardiovascular Imaging Inc].

2.2 | Data analysis

The real-time MR images, binned into eight respiratory categories, were analyzed regarding the benefit of respiratory binning for motion control, the left ventricular EI, and the respiratory effects on the ventricular volumes.

2.3 | Motion control

To quantify the quality of motion control, the displacement of the middle—between the cranial and the caudal end of the interventricular septum (Figure 2A,B)—was determined in a midventricular slice for all respiratory categories (eight heartbeats). Anterior-to-posterior (right-to-left) movement (Figure 2A), superior-to-inferior (left anterior to right posterior) displacement (Figure 2B) and rotation were analyzed separately. Images solely sorted based on ECG and images sorted by data from ECG and respiratory bellows served for comparison.

2.4 | Left ventricular eccentricity index

The left ventricular EI was determined in the series overview module from cardiac MRI software cvi 42 (Circle Cardiovascular Imaging Co). It was analyzed for all end-diastolic and end-systolic phases of a midventricular slice. The evaluation was performed separately for endocardial and epicardial contours and calculated from the horizontal diameter (perpendicular to the septum) and vertical diameter (parallel to the septum; Figure 3).

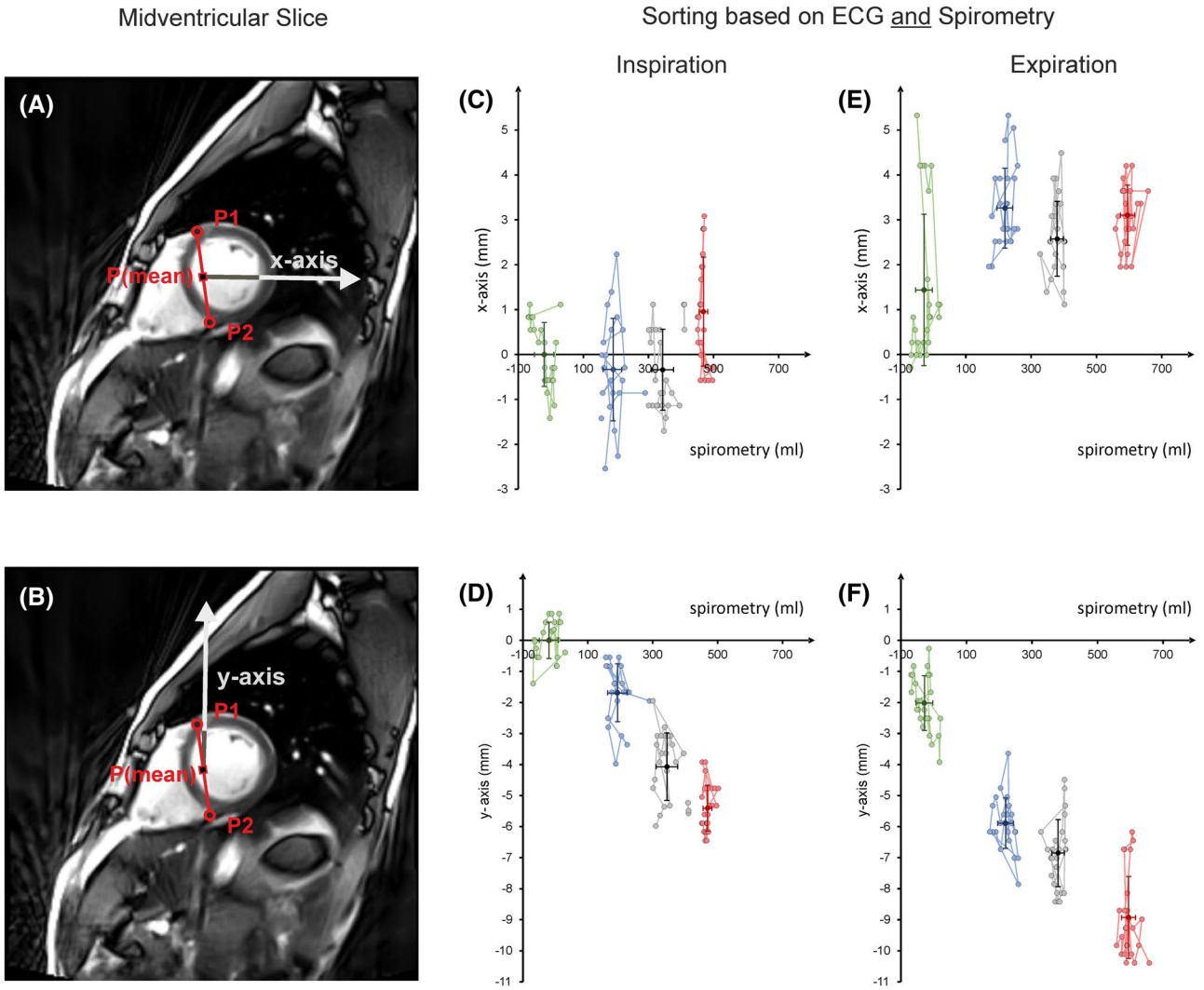

FIGURE 2 Motion control. The middle between the cranial (P1) and caudal (P2) junction of the interventricular septum with the right ventricle P (mean) served as reference point (A,B) for the analysis of motion control. The movement in horizontal direction (x-axis; A,C,E) and vertical direction (y-axis; B,D,F) was calculated referring to the defined point in a heart cycle. The reference point remained quite stable in heart cycles composed of images sorted by electrocardiogram and spirometry volume (C-F)

2.5 | Volumetry

Ventricular volumes were calculated for each respiratory category with the Short3D module of the cardiac MRI software cvi 42 (Circle Cardiovascular Imaging Co). Manual corrections were performed (L.R.) using a standardized approach (see Supporting Information S4) based on current recommendations on image analysis[15-18] (see also Supporting Information Video S1).

2.6 | Statistical analysis

Statistical analysis was calculated using SPSS Statistics for Windows (version 25.0, released 2017; IBM Corp).

The Shapiro-Wilk test was used to test for normal distribution. In case of nonnormal distribution (eg, motion control), the nonparametric Wilcoxon matched-pair test and the Kruskal-Wallis test were used where appropriate.

Linear regression was performed to evaluate the correlation between the spirometry volume and the corresponding volumes and the influence of the spirometry volume on the left ventricular EI.

$P < .05$ was considered statistically significant.

3 | RESULTS

3.1 | MR-compatible spirometry

Subjects breathed freely and evenly with a respiratory rate of 13.5 ± 1.4 per minute and a tidal volume of 9.9 ± 3.8 mL/kg, resulting in a respiratory minute volume of 125.6 ± 38.4 mL/kg/min ($n = 4$). A questionnaire (Supporting Information S3) showed that the subjects' degree of anxiety was hardly influenced by spirometry, and the overall comfort with connected spirometry was still high (see Supporting Information S3 for details).

3.2 | Binning

Whereas ECG bins were filled almost evenly, spirometry binning showed a nonuniform distribution with considerably less images assigned to the intermediate respiratory classes. Consequently, the number of images necessary to fill the majority of bins was approximately four- to fivefold the number of bins (see Supporting Information S5, Table S1, Figure S3).

3.3 | Motion control

Binning of images that was solely based on the ECG phase, but without considering the respiratory category, resulted in blurred sequences hardly useful for qualitative, visual assessment ("eyeballing"; Supporting Information Video S2, first part). Combining binning for ECG phase with binning by spirometry or respiratory bellows improved motion control meaningfully (Figure 2; Supporting Information Video S2, second and third parts). The superiority of spirometry over respiratory bellows could not be shown (see Supporting Information S6, Table S2, and Figure S4 for details).

3.4 | Left ventricular eccentricity index

The impact of an increasing lung volume on the left ventricular end-diastolic eccentricity index (EId) was obvious (Figure 3C,E) with a higher index with increasing lung volume during inspiration (Figure 3C), as well as expiration (Figure 3E), whereas there was no effect on the end-systolic left ventricular eccentricity index (EIs; Figure 3D,F).

3.5 | Respiration-dependency of ventricular volumes

Respiration had a relevant impact on the shape and volumes of both ventricles.

3.5.1 | Right ventricle

Qualitative analysis

At end-diastole (Supporting Information Video S3, first part) the size of the right ventricle increases during inspiration. Although at the end of expiration the ventricle has got an almost triangular shape, it becomes more convex and rounded with inspiration. Both effects are less pronounced at end systole (Supporting Information Video S3, second part).

Quantitative analysis

The right ventricular end-diastolic volume (RV-EDVi), stroke volume (RV-SVi), and RV-EF increased especially during inspiration, whereas the end-systolic volume (RV-ESVi) remained almost unchanged (Figure 4, Supporting Information Figure S5). This was paralleled by an increase of the RV-SVi (Figure 4) and an increase of the RV-EF.

The mean increases of the right ventricular volumes referenced to the increase of the lung volume during inspiration were RV-EDVi approximately 3.6 mL/m^2, that is, approximately 5% per 100-mL lung volume, RV-SVi approximately 3.3 mL/m^2, that is, approximately 8% per 100-mL lung volume.

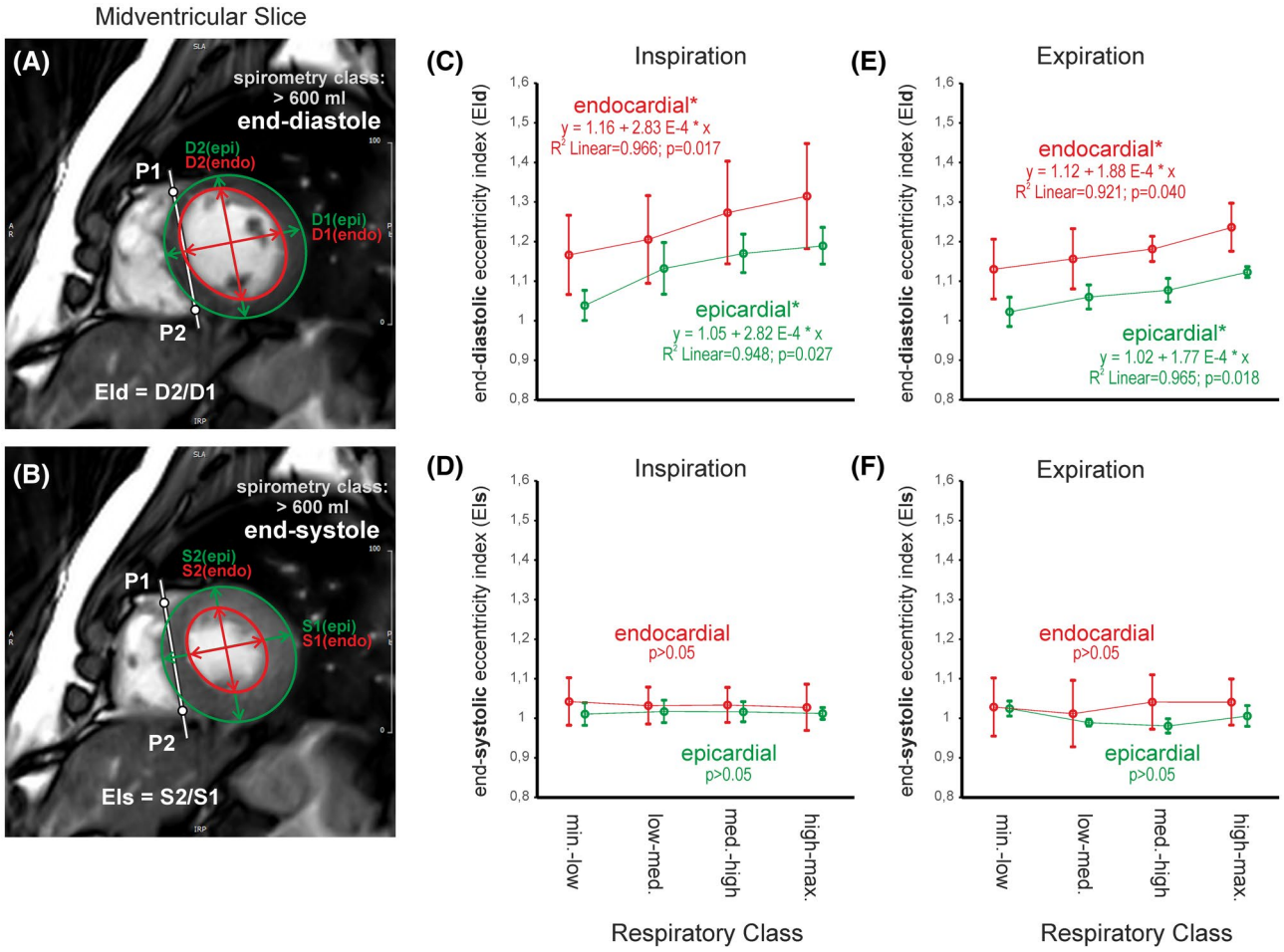

FIGURE 3 Eccentricity index. The left ventricular eccentricity index (EI) was calculated for end-diastole (EId) (A) and end-systole (EIs) (B) for the endocardial (red) and epicardial (green) border of the midventricular slice by calculating the ratio of the axis parallel to the interventricular septum (D2, S2) to the axis perpendicular to the interventricular septum (D1, S1). Whereas the end-diastolic left ventricular eccentricity index (EId) increased with a higher lung volume during inspiration (C,D), as well as during expiration (E,F), the end-systolic left ventricular eccentricity index (EIs) is not influenced by respiration (D,F). Circles indicate mean value, whiskers, and standard deviation. $*P < .05$ (linear regression). Results of the corresponding linear regression analyses are inserted in the graphs in case of statistical significance. The unit of x in the linear equations is milliliters of lung volume

3.5.2 | Left ventricle

Qualitative analysis

At end diastole, the shape of the left ventricle turns from a circle to an ellipse during inspiration (Supporting Information Video S3, first part), the effect on the size of the left ventricle (decreasing diameter during inspiration) is less obvious. The shape remains unaffected by respiration at end systole (Supporting Information Video S3, second part).

Quantitative analysis

Left ventricular end-diastolic volume (LV-EDVi), left ventricular stroke volume (LV-SVi), and left ventricular EF (LV-EF) decreased during inspiration, while the left ventricular end-systolic volume (LV-ESVi) increased (Figure 4, Supporting Information Figure S5). The decrease of LV-EDVi, LV-SVi, and LV-EF were less pronounced compared with the respiratory impact on the right ventricular volumes.

3.6 | Frank-Starling law

There were highly significant linear relationships between SVi and EDVi whenever there was a significant change of the ventricular volume (ΔEDVi > 5 mL/m^2; see Figure 5). The slopes for the Frank-Starling law-related curves for the right ventricle during inspiration (ΔRV-SVi/ΔRV-EDVi) were 0.9 for inspiration and expiration (Figure 5A); the slope for the left ventricle (ΔLV-SVi/ΔLV-EDVi) was 1.1 (Figure 5B).

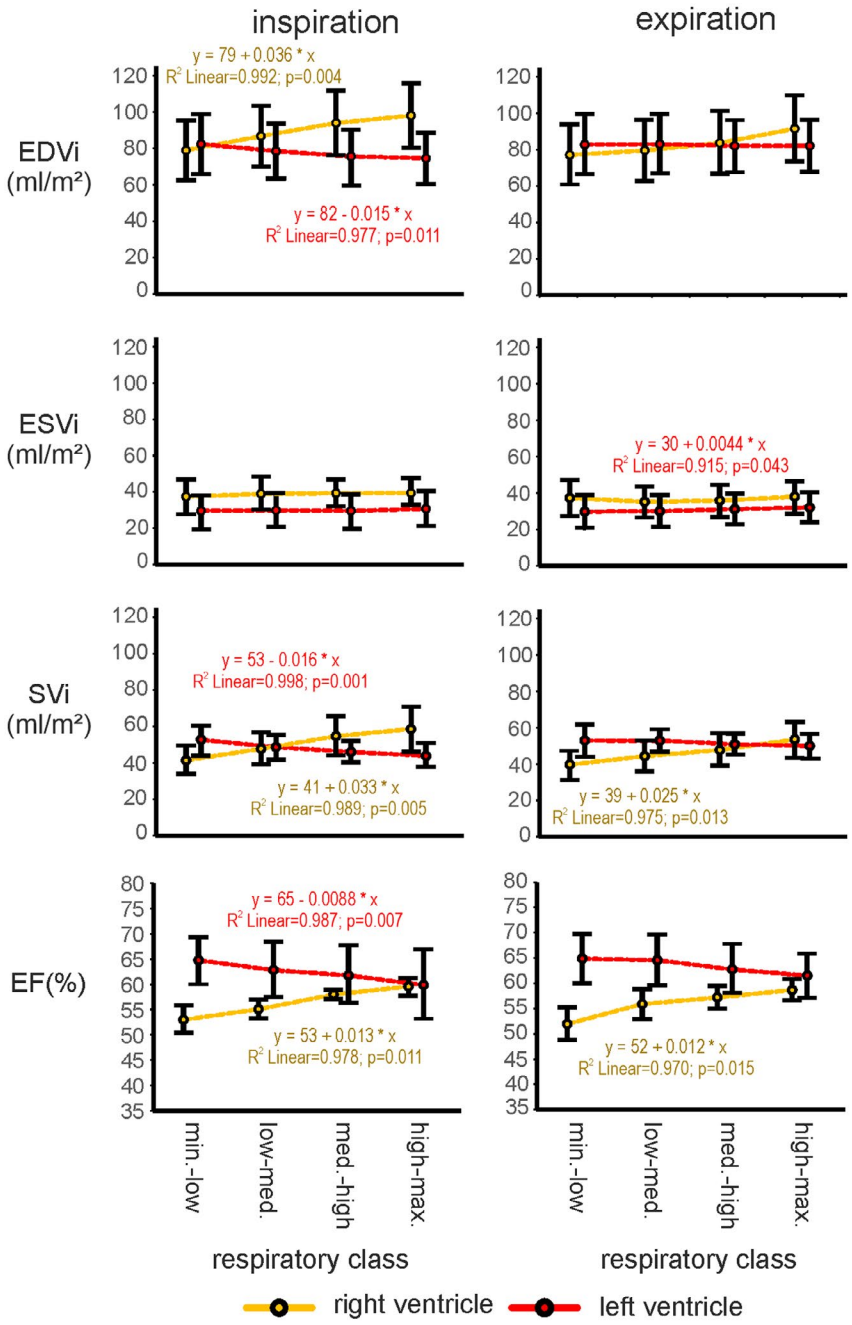

FIGURE 4 Volumetry. The mean values (± standard deviation) of the end-diastolic volume (EDVi), the end-systolic volume (ESVi), the stroke volume (SVi), and the ejection fraction (EF) for the left and right ventricles indexed to the body surface area were shown for all respiratory categories. The results of the corresponding linear regression analyses are inserted in the graphs in case of statistical significance ($R^2 > 0.96$; $P \leq .015$). The lung volume measured by spirometry as a continuous numerical variable instead of respiratory categories was preferred for linear regression analyses (the unit of x was in milliliters)

4 | DISCUSSION

We started a proof-of-principle study to show the possibility of performing real-time cardiac MRI during free-breathing using respiratory gating with MR-compatible spirometry maintaining bona fide physiological conditions. We expected improved motion control, resulting in a less error-prone semiautomated image analysis. In addition to the original goals the method turned out to be a tool that can provide data on basic cardiac physiology and heart–lung interactions.

We used spirometry because it is the gold-standard technique for assessing pulmonary ventilatory function in humans quantitatively. Binning is a technique frequently used for motion compensation (eg, Shahzadi et al[19]). We used binning to group the images according to RR interval and spirometry signals into data classes, that is, "bins." The number of bins determines the similarity of the images with respect to RR interval and lung volume and is crucial for the required number of images. We decided to differentiate between inspiration and expiration because our results and the results of previous studies[2,20] have shown relevant functional differences.

We found that for 18,000 images, a recording time of 10 minutes was required to fill all bins (20 image planes × 25 ECG classes × four breathing categories × inspiration/expiration = 4000 bins) sufficiently. Thus, the number of images required 4 to 5 times the number of bins.

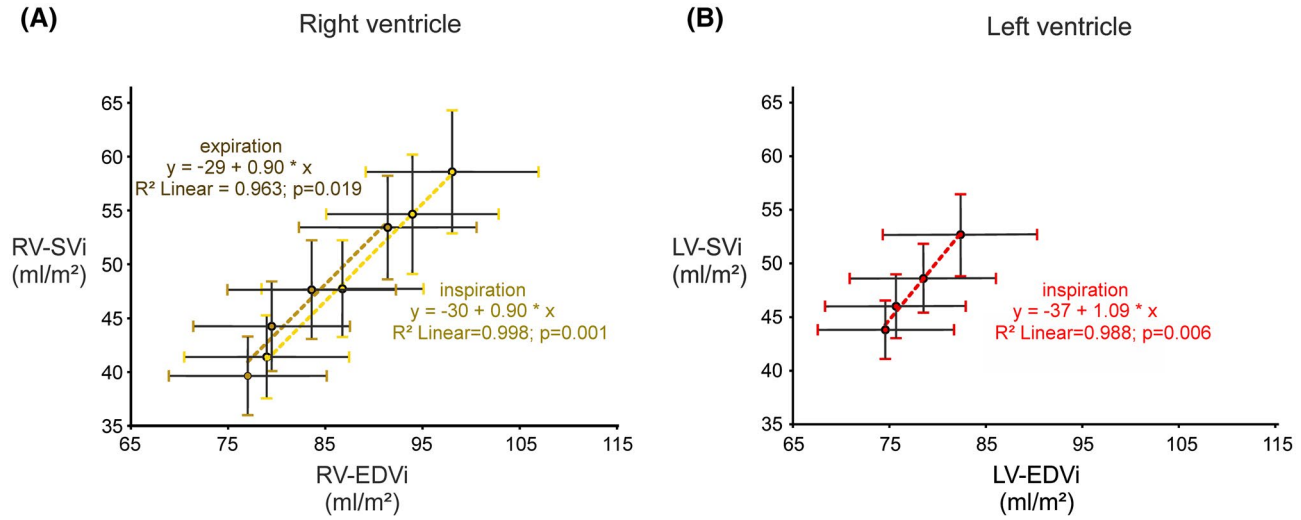

FIGURE 5 Frank-Starling mechanism. When the end-diastolic volume (EDVi) of the ventricles was modified significantly by respiration (ΔEDVi > 5 mL/m^2), the relationship between stroke volume (SVi) and EDVi could be analyzed. Linear regression revealed highly significant relationships for (A) the right ventricle (RV), and (B) the left ventricle (LV) during inspiration. Circles indicate mean value, whiskers, standard error of the mean. *$P < .05$ (linear regression). The unit of x in the linear equations was mL/m^2

Although standard gating techniques during cine imaging select only one respiratory class, typically the end of expiration, we obtained images in every respiratory class.

The intriguing aspect about this approach is that by rearranging the images, we were able to study these images in a completely novel way: Although the classical approach is to control for respiration and to analyze the change of the heart during a heart cycle, we had the opportunity to control for the heart cycle and analyze the cardiac alterations of the heart during a respiratory cycle.

Respiratory motion during cardiac MRI has at least three different aspects. First, motion may result in blurry images. The easiest way to solve this problem is to eliminate respiratory motion by breath-hold imaging. Apart from the fact that long phases without breathing are problematic for many patients,[21,22] holding one's breath is unphysiological and has an influence on function and the dimensions of both ventricles.[1-3] We chose accelerated imaging by real-time MRI, which is an alternate, more physiological approach.

The second aspect of respiratory motion is its impact on image analysis. Because of the respiratory motion of the heart, the quantitative assessment of the large number of images acquired with the help of real-time sequences becomes difficult and time-consuming. Stabilization of videos for image analysis is provided by respiratory binning, but can be achieved with increasing the quality using appropriate software, too.

The most important aspect, however, is respiratory motion as an expression of pulmonary function, which induces heart–lung interactions. Therefore, beyond image stabilization, maintaining respiratory information is highly desirable.

Various techniques for registering respiration have been developed over the last few decades (see Runge et al[23] for a review on respiratory gating). Frequently, respiratory gating is based on respiratory bellows, recording the movement of the thorax or abdomen, or navigator echoes, reflecting the position of the diaphragm.[24]

Navigator echoes would have interrupted real-time MRI. Indirect respiratory measurement via bodily movement by respiratory bellows is artifact-prone and not quantitative.[24]

Our results show that during regular breathing, retrospective gating was possible by respiratory bellows, as well as by MR-compatible spirometry. The limiting factor for the quality of image stabilization is the number of respiratory classes. Increasing the number of respiratory bins, however, would have increased scan time significantly.

Although motion reduction is possible with both techniques, an exact assignment of the image data to specific lung volumes is only possible with the help of spirometry. The latter is, therefore, the prerequisite for the analysis of the heart–lung interactions described.

To test the hypothesis that the described combination of real-time MRI, spirometry, and binning is suited to examine the respiratory influence on cardiac parameters, we analyzed whether the effect of spontaneous breathing on ventricular shape, function, and dimensions shown by other, particularly invasive techniques, could be reproduced noninvasively with this setup.

First, the effect of respiration on cardiac function was assessed by the left ventricular EI. The position of the ventricular septum is influenced by right ventricular pressure and volume load.[25] An increase in the EIs indicates an increased right ventricular pressure, whereas the EId serves as a marker for an increased right ventricular volume load.[25] As expected, the EIs did not change in our healthy subjects not suffering from, for example, pulmonary hypertension. However, the

EId was significantly influenced by respiration; it was minimal at the end of expiration and maximal at the end of inspiration, indicating an increased volume load during inspiration.

Though easy to obtain, given the respiratory-induced through-plane motion of the heart, a simple assessment of one midventricular slice does not replace true volumetry. This, however, is provided by the analysis of sorted images.

Binning of images of all slices according to the respiratory phases resulted in eight stacks of images that could be processed similar to the images obtained during breath-holding at different phases during the respiratory cycle.

The first result was that even during spontaneous breathing, the volumes of the right and left ventricle changed significantly. This reinforces the observation from previous studies that the mixing of images acquired during different respiratory situations is inadequate.[2]

During inspiration, the right ventricular end-diastolic volume increases. This observation is perfectly supported by previous physiological studies[26-28] and can be explained primarily by a change of the ventricular preload (see Magder[2] for a review).

In contrast, there is a decrease of the left ventricular end-diastolic volume during inspiration. This has long been known and has been well described using different methods.[2,28] The mechanism thereof is difficult to discern.[2,29-31] Most likely, it is a consequence of a decrease of left ventricular compliance and an increased afterload.[2,31,32]

Our results show respiratory-induced changes of the end-diastolic volumes of both ventricles. This gave us the unique opportunity to study one of the most fundamental concepts of human physiology, the Frank-Starling mechanism.

The Frank-Starling law describes an increase of stroke volume with increasing end-diastolic volume (see Delicce and Makaryus[33] for a review).

We could show that the respiratory-induced changes of the end-diastolic volume during normal breathing modified the stroke volume as predicted by the Frank-Starling law.[34,35] We are not aware of any previous publication that could quantify this relationship noninvasively and under physiological conditions, and correlate this with the increase in lung volume. Such values should be helpful for understanding and modeling heart–lung interactions.

The present work shows the feasibility of the method and was able to show that it is suitable for providing quantitative and potentially clinically relevant data on heart–lung interactions. However, to apply the methodology, first scientifically and then clinically, the number of cases would have to be increased considerably, standardization should be improved, and the study protocol will have to be optimized. In addition, although MR-compatible spirometry was well tolerated and is currently the gold standard for measuring lung function and will probably remain so, an alternate, even more comfortable noninvasive technique that could provide quantitative respiratory data would be desirable.

5 | CONCLUSIONS

Real-time MRI during spontaneous breathing in combination with MR-compatible spirometry and retrospective binning provides image stabilization, allows quantitative image analysis, and most interestingly offers unique opportunities to assess heart–lung interactions.

ACKNOWLEDGMENT

The authors thank Evelyn Radomsky for the exceptional technical assistance, Julia Camilleri for her statistical advice, Jeanette Schulz-Menger for her discussion of our contouring manual, Hans-Jörg Wittsack for insightful discussions and technical support, and Marcus Welsh for his writing assistance. Finally, the generous financial assistance of the Elterninitiative Kinderkrebsklinik e.V. is hereby acknowledged.

DATA AVAILABILITY STATEMENT

The code and an example of a data set that serves to demonstrate the code are openly available (https://doi.org/10.5281/zenodo.4899285).

ORCID

Jens Frahm https://orcid.org/0000-0002-8279-884X
Frank Pillekamp https://orcid.org/0000-0003-1968-8944

REFERENCES

1. Ferrigno M, Hickey DD, Linér MH, Lundgren CE. Cardiac performance in humans during breath holding. *J Appl Physiol*. 1986;60:1871-1877.
2. Magder S. Heart-Lung interaction in spontaneous breathing subjects: the basics. *Ann Transl Med*. 2018;18:348.
3. Paulev P, Wetterqvist H. Cardiac output during breath-holding in man. *Scand J Clin Lab Invest*. 1968;22:115-123.
4. Scott AD, Keegan J, Firmin DN. Motion in cardiovascular MR imaging. *Radiology*. 2009;250:331-351.
5. Uecker M, Zhang S, Voit D, Karaus A, Merboldt KD, Frahm J. Real-time MRI at a resolution of 20 ms. *NMR Biomed*. 2010;23:986-994.
6. Voit D, Zhang S, Unterberg-Buchwald C, Sohns JM, Lotz J, Frahm J. Real-time cardiovascular magnetic resonance at 1.5 T using balanced SSFP and 40 ms resolution. *J Cardiovasc Magn Reson*. 2013;15:79.
7. Frahm J, Voit D, Uecker M. Real-time magnetic resonance imaging: radial gradient-echo sequences with nonlinear inverse reconstruction. *Invest Radiol*. 2019;54:757-766.
8. Zhang S, Joseph AA, Voit D, et al. Real-time magnetic resonance imaging of cardiac function and flow-recent progress. *Quant Imaging Med Surg*. 2014;4:313-329.
9. Bauer RW, Radtke I, Block KT, et al. True real-time cardiac MRI in free breathing without ECG synchronization using a novel sequence with radial k-space sampling and balanced SSFP contrast mode. *Int J Cardiovasc Imaging*. 2013;29:1059-1067.
10. Eichinger M, Puderbach M, Smith H-J, et al. Magnetic-resonance-compatible-spirometry: principle, technical evaluation and application. *Eur Respir J*. 2007;30:972-979.

11. Kokki T, Klén R, Noponen T, et al. Linear relation between spirometric volume and the motion of cardiac structures: MRI and clinical PET study. *J Nucl Cardiol*. 2016;23:475-485.
12. Chen S, Hu P, Gu Y, et al. Impact of patient comfort on diagnostic image quality during PET/MR exam: a quantitative survey study for clinical workflow management. *J Appl Clin Med Phys*. 2019;20:184-192.
13. Harris CR, Millman KJ, van der Walt SJ, et al. Array programming with NumPy. *Nature*. 2020;585:357-362.
14. Mason D, scaramallion, rhaxton, et al. Pydicom/pydicom: V1. 4. 0. January 20, 2020. Zenodo. Available at: https://doi.org/10.5281/zenodo.3614042. Accessed September 15, 2020.
15. Schulz-Menger J, Bluemke DA, Bremerich J, et al. Standardized image interpretation and post processing in cardiovascular magnetic resonance: society for cardiovascular magnetic resonance (SCMR) board of trustees task force on standardized post processing. *J Cardiovasc Magn Reson*. 2013;15:35.
16. Paknezhad M, Marchesseau S, Brown MS. Automatic basal slice detection for cardiac analysis. *J Med Imaging (Bellingham)*. 2016;3:034004.
17. Marchesseau S, Ho JXM, Totman JJ. Influence of the short-axis cine acquisition protocol on the cardiac function evaluation: a reproducibility study. *Eur J Radiol Open*. 2016;3:60-66.
18. van der Ven JPG, Sadighy Z, Valsangiacomo Buechel ER, et al. Multicentre reference values for cardiac magnetic resonance imaging derived ventricular size and function for children aged 0–18 years. *Eur Heart J Cardiovasc Imaging*. 2020;21:102-113.
19. Shahzadi I, Siddiqui MF, Aslam I, Omer H. Respiratory motion compensation using data binning in dynamic contrast enhanced golden-angle radial MRI. *Magn Reson Imaging*. 2020;70:115-125.
20. Dasari P, Johnson K, Dey J, et al. MRI investigation of the linkage between respiratory motion of the heart and markers on patient‘s abdomen and chest: implications for respiratory amplitude binning list-mode PET and SPECT studies. *IEEE Trans Nucl Sci*. 2014;61:192-201.
21. Gay SB, Sistrom CL, Holder CL, Suratt PM. Breath-holding capability of adults. Implications for spiral computed tomography, fast-acquisition magnetic resonance imaging, and angiography. *Invest Radiol*. 1994;29:848-851.
22. Funk E, Thunberg P, Anderzen-Carlsson A. Patients' experiences in magnetic resonance imaging (MRI) and their experiences of breath holding techniques. *J Adv Nurs*. 2014;70:1880-1890.
23. Runge VM, Richter JK, Heverhagen JT. Motion in magnetic resonance: new paradigms for improved clinical diagnosis. *Invest Radiol*. 2019;54:383-395.
24. Santelli C, Nezafat R, Goddu B, et al. Respiratory bellows revisited for motion compensation: preliminary experience for cardiovascular MR. *Magn Reson Med*. 2011;65:1097-1102.
25. Ryan T, Petrovic O, Dillon J, Feigenbaum H, Conley MJ, Armstrong WF. An echocardiographic index for separation of right ventricular volume and pressure overload. *J Am Coll Cardiol*. 1985;5:918-927.
26. Guyton AC, Lindsey AW, Abernathy B, Richardson T. Venous return at various right atrial pressures and the normal venous return curve. *Am J Physiol*. 1957;189:609-615.
27. Shuler RH, Ensor C, Ginning RE, Moss WG, Johnson V. The differential effects of respiration on the left and right ventricles. *Am J Physiol*. 1942;137:620-627.
28. Claessen G, Claus P, Delcroix M, Bogaert J, La Gerche A, Heidbuchel H. Interaction between respiration and right versus left ventricular volumes at rest and during exercise: a real-time cardiac magnetic resonance study. *Am J Physiol Heart Circ Physiol*. 2014;306:H816-H824.
29. Korperich H, Barth P, Gieseke J, et al. Impact of respiration on stroke volumes in paediatric controls and in patients after Fontan procedure assessed by MR real-time phase-velocity mapping. *Eur Heart J Cardiovasc Imaging*. 2015;16:198-209.
30. Ruskin J, Bache RJ, Rembert JC, Greenfield JC Jr. Pressure-flow studies in man: effect of respiration on left ventricular stroke volume. *Circulation*. 1973;48:79-85.
31. Wise RA, Robotham JL, Summer WR. Effects of spontaneous ventilation on the circulation. *Lung*. 1981;159:175-186.
32. Summer WR, Permutt S, Sagawa K, Shoukas AA, Bromberger-Barnea B. Effects of spontaneous respiration on canine left ventricular function. *Circ Res*. 1979;45:719-728.
33. Delicce AV, Markaryus AN. *Physiology, Frank Starling Law*. In: StatPearls. Treasure Island (FL): StatPearls Publishing; 2020.
34. Frank O. Zur Dynamik des Herzmuskels. *Ztschr Biol*. 1895;32:370.
35. Starling EH. The linacre lecture on the law of the heart. Given at Cambridge, 1915. *Nature*. 1918;101:1–27.

SUPPORTING INFORMATION

Additional Supporting Information may be found online in the Supporting Information section.

VIDEO S1 Contouring Video. Video demonstrating the contouring of all slices of a completely reconstituted heart cycle for the volume category "minimum–low / inspiration." Contours were corrected manually after automatic detection

VIDEO S2 Motion Control. The first part of the video shows a basal to midventricular slice of a heart cycle of a reconstruction based only on the ECG phase. There is a pronounced movement of the heart because of different respiratory conditions. In contrast, the second part of the video demonstrates the same slice of the same subject when only images of one spirometry class (inspiration, volume <150 mL) were chosen. The third part of the video shows an equivalent heart cycle sorted with respiratory bellows (inspiration, resp. bellows a.u. <1000). The improvement of motion control in heart cycles with respiratory detection with spirometry or respiratory bellows is obvious

VIDEO S3 Heart-lung interactions. Respiratory-induced variation of cardiac morphology during two ECG-defined phases of the cardiac cycle in a healthy volunteer during spontaneous breathing: In both ECG-defined cardiac phases a higher spirometry-determined lung volume (spirometry class, ie, lung volume above baseline) is associated with an increased lung area, caudal displacement of heart and liver, and an increased right ventricular area. First part of the video: end-diastole (45 ± 11 ms after R wave). The shape of the left ventricle becomes eccentric and changes from a circle to an ellipse with increasing lung volume during inspiration. Second part of the video: end-systole (406 ± 12 ms after R wave). The left ventricle remains round

FIGURE S1 Imaging Protocol. (A) Continuous real-time MR images (~36 images/heartbeat) were recorded simultaneously

with spirometry (middle row) and ECG (lower row). (B) To cover the whole heart, 20 slices were sequentially acquired resulting in a scan time of 10 minutes (corresponding to 30 s/slice and 900 images/slice)

FIGURE S2 MR-compatible spirometry. (A) Schematic diagram of MR and MR-compatible spirometry set-up. (B) Photograph of the spirometry set-up taken outside the MR scanner room

FIGURE S3 Distribution. Example demonstrating the distribution of the images to the ECG classes (A-C), respiratory classes (D-F). ECG. The number of images is almost evenly distributed up to mean RR interval (A, B) resulting in a similar percentage of filled ECG classes (C, green). Respiratory Classes. More imaging time is spent in the extreme respiratory classes (D, E). Consequently, the number of unfilled classes (F, red) is higher in the intermediate classes

FIGURE S4 Motion Control. The middle between the cranial (P1) and caudal (P2) junction of the interventricular septum with the right ventricle P(mean) served as reference point (A, B) for the analysis of motion control. The movement in horizontal direction (x-axis) (A, C, E, G, I, K) and vertical direction (y-axis) (B, D, F, H, J, L) was calculated referring to the defined point in a heart cycle. Solely ECG sorted images (C, D) demonstrated a largely irregular position, whereas the reference point remained quite stable both in heart cycles composed of images sorted by ECG and spirometry volume (E-H) or ECG and respiratory bellows (I-L)

FIGURE S5 Volumetry. The mean values (±SD) of the end-diastolic volume, the end-systolic volume, the stroke volume, and the ejection fraction for the left and right ventricle indexed to the body surface area were demonstrated for all respiratory categories on the left. The right part demonstrates the mean values (±SD) of the end-diastolic volume, end-systolic volume, stroke volume and the ejection fraction for the left and right ventricle relative to the mean results of the lowest volume class for all respiratory categories. Results of the corresponding linear regression analyses are inserted in the graphs in case of statistical significance ($R^2 > 0.96$; $P \leq .015$). The lung volume measured by spirometry as a continuous numerical variable instead of respiratory categories was preferred for linear regression analyses (unit of x: ml)

TABLE S1 Distribution. (A) More images were assigned to the extreme spirometry classes ("minimum-low" & "high-maximum" lung volume) as compared to the intermediate classes ("low-medium" & "medium-high" lung volume) resulting in a lower percentage of filled classes in the latter. (B) Images were almost evenly distributed among the ECG classes with a homogeneously high percentage of filled classes

TABLE S2 Motion Control Tables. Motion analysis of the midventricular slice of the four subjects. The tables provide data on the movement of the heart during breathing ("mean position and angulation") and on the motion of the heart between subsequent images ("mean displacement and rotation"). Mean displacement is reduced significantly by respiratory binning, either by spirometry or by respiratory bellows

DOCUMENT S1 Imaging protocol. Detailed information on the imaging protocol and information on ECG and respiratory bellows data acquisition

DOCUMENT S2 MR-compatible spirometry. Additional information on the function and technical background of MR-compatible spirometry

DOCUMENT S3 Questionnaire. (A) Comfort and anxiety questionnaire (modified from Chen S et al. 2018). (B) Results of the evaluation of this questionnaire for the four subjects

DOCUMENT S4 Contouring Manual. Relevant sections of the contouring manual: (A) Definition of the apical slice of the short axis stack. (B) Dealing with papillary muscles. (C) Definition of the basal slice of the short axis stack. (D) Definition of the end-diastolic and end-systolic phase

DOCUMENT S5 Binning Results. Detailed results of binning with ECG and MR-compatible spirometry

DOCUMENT S6 Motion Control Results. Detailed results of the Motion control analysis

How to cite this article: Röwer LM, Uelwer T, Hußmann J, et al. Spirometry-based reconstruction of real-time cardiac MRI: Motion control and quantification of heart–lung interactions. *Magn Reson Med*. 2021;86:2692–2702. https://doi.org/10.1002/mrm.28892